 DOI: 10.1002/masy.201300106

Effect of Surface Morphology of Poly(ε-caprolactone) Scaffolds on Adipose Stem Cell Adhesion and Proliferation

Nazely Diban,[1,2] *Suvi P. Haimi*,[2,3] *Lydia Bolhuis-Versteeg*,[2] *Sandra Teixeira*,[2] *Susanna Miettinen*,[3] *André A. Poot*,[2] *Dirk W. Grijpma*,[2,4] *Dimitrios Stamatialis**[2]

Summary: The effect of the surface morphology of flat poly(ε-caprolactone) (PCL) scaffolds on human adipose stem cell (hASC) adherence and proliferation was studied. During fabrication of the scaffolds by phase inversion, the employment of different non-solvents (water (W), ethanol (EtOH) or isopropanol (IPA)) led to distinct surface morphologies. It was found that PCL scaffolds fabricated using IPA as a non-solvent had a higher roughness and porosity compared to the other groups. Moreover, during culturing of hASCs under static conditions, best cell attachment, spreading and growth were observed on the PCL scaffold. Our results show the potential of PCL scaffolds prepared using IPA as a non-solvent for especially soft tissue engineering applications.

Keywords: morphology; phase inversion; poly(ε-caprolactone); scaffold porosity; roughness

Introduction

Tissue engineering (TE) involves porous scaffolds to act as templates and guides for cell proliferation, differentiation and tissue growth in order to regenerate living tissues.[1] The scaffold surface morphology, together with other substrate stimuli, such as material stiffness, elasticity and chemistry, strongly influence the cell-substrate interaction and cellular response.[2–3] The influence of micro- and nano-topography (i.e. grooves and ridge patterns) on cell adhesion, migration, proliferation or differentiation has already been widely covered in the literature.[4–5] Certain physical parameters related to the scaffold morphology, such as porosity, pore size and roughness, have been shown to differently affect the cues for cell response depending on the type of cells[6] and surface materials used.[7] Some of the techniques employed to alter the surface morphology of a scaffold include micromolding,[4–5] doping micro- or nano-particles[8–10] (with or without subsequent particle leaching), grafting biomolecules,[11–12] or treatment of the scaffold surfaces either chemically[6,13] or physically.[14] Moreover, earlier studies showed that phase inversion, a rapid and cheap method for scaffold fabrication, can also be successfully applied.[5,15–17]

Poly(ε-caprolactone) (PCL) is a biodegradable and biocompatible polymer, broadly employed in biomedical and TE applications, with interesting mechanical properties and degradation rates to preserve the necessary mechanical properties of the scaffold *in vivo* over time until the cellular tissue has been reconstituted.[18–19] The crystalline structure of PCL is beneficial for regeneration of hard tissues such as bone, but limits its applications for engineering of soft tissues. Interestingly,

[1] Department of Chemical Engineering, University of Cantabria, Spain
[2] Biomaterials Science and Technology/MIRA Institute, University of Twente, The Netherlands
E-mail: D.Stamatialis@utwente.nl
[3] Adult Stem Cells/Institute of Biomedical Technology, University of Tampere, Finland
[4] Department of Biomedical Engineering, University Medical Center Groningen and University of Groningen, The Netherlands

modification of the surface roughness of PCL scaffolds on the nanoscale by grafting biomolecules was found to promote the growth of endothelial and fibroblast cells.[11–12] In an earlier study,[20] we developed flat PCL scaffolds by phase inversion with different surface morphologies tailored by employing different solvent/non-solvent combinations. Particularly, PCL scaffolds fabricated using N-methylpyrrolidone (NMP) as a solvent presented potential surface morphologies for the promotion of cell organization. In this work, human adipose stem cells (hASCs) were used to elucidate the effect of PCL surface morphology on cell attachment and proliferation. These multipotent mesenchymal stem cells are an abundant and easy source of cells for several tissue engineering applications since they can differentiate towards several lineages, e.g. endothelial, myogenic and adipogenic lineages, when cultured under specific conditions.[21–23]

Materials and Methods

Scaffold Preparation

Flat PCL scaffolds were prepared by phase inversion following the procedure described elsewhere.[20] Briefly, PCL (MW 80 kDa, Sigma Aldrich, Steinheim, Germany) polymer solution of 15% w/w was prepared by dissolving PCL under stirring in NMP (99% purity, Acros Organics, Geel, Belgium) at 40 °C during 24 h. The polymer solution was filtered through a 25 μm metallic mesh filter under pressure and was left to degas overnight. The polymer solution was cast at room temperature on a glass plate using a 0.2 mm thickness casting knife and immediately submerged into the coagulation bath composed of either Milli-Q water (W), ethanol (EtOH, analytical grade, Merk) or 2-propanol (IPA, AR, Biosolve BV). The glass plate with the polymer scaffold was kept in the coagulation bath until the scaffold was spontaneously released from the glass plate. Then, the scaffold was placed into a new coagulation bath to complete the solvent exchange during 24 h. In order to ensure complete removal of solvent traces, the scaffolds were subsequently immersed in water cleaning baths changed periodically during 48 h. This washing procedure was proven sufficient for complete NMP removal in other studies.[16–17] The casting/coagulation procedure was repeated 3 times for each non-solvent or coagulation bath (W, EtOH and IPA) designated with scaffold code PCL/W, PCL/EtOH or PCL/IPA, respectively.

Evaluation of Cell Culture and Cell Viability on PCL Scaffolds

Cell Culture

For the cell culture experiments, flat scaffolds were cut into square pieces of 1×1 cm size ($\sim$1 cm^2 external surface area and thickness of the scaffolds ranging from 98 to 143 μm[20]). Each sample was sterilized with 70% v/v EtOH in distilled water for 30 min, and then EtOH was allowed to evaporate for another 30 min. After sterilization, the samples were washed 6 times with Dubelcco's Phosphate Buffered Saline (DPBS; Invitrogen, Paisley, UK) and finally pretreated with maintenance medium consisting of Dulbecco's Modified Eagle Medium/F-12 (1:1) with HEPES and L-Glutamine (Invitrogen, CA, USA), 10% human serum type AB (PAA Laboratories GmbH, Pasching, Austria) and 1% antibiotics (100 U/mL penicillin and 100 μg/mL streptomycin; Invitrogen) for 48 h at 37 °C.

The protocols for hASCs isolation, expansion and the flow cytometric expression analysis of the surface markers were described in previous reports.[16–17] Each flat scaffold was seeded with 100 000 cell/cm^2 in 25μL of maintenance medium. The cells were allowed to attach to the scaffolds for 3 h at 37°C before adding final medium volume (975 μL) to the 24-well plates. The cell-seeded scaffolds were cultured under static conditions for 7 days and the maintenance medium was exchanged every other day. Static culturing experiments were performed in triplicates in all cases.

Cell Attachment and Viability

Attachment and viability of hASCs were studied at days 1 and 7 using a LIVE/DEAD® Viability/Cytotoxicity Assay Kit (Invitrogen) according to the manufacturer's protocols. The viable cells (green fluorescence) and necrotic cells (red fluorescence) were visualized using a fluorescence microscope (Eclipse E600, Nikon, Japan).

The cell-seeded membranes were stained with Methylene Blue (MB) (Sigma Aldrich, Steinheim, Germany) staining at days 1 and 7 in order to evaluate cell morphology and spreading. Briefly, the membranes were washed with DPBS, and cells were fixed with 1.5% glutaraldehyde (Glutaraldehyde 25%, aqueous solution, (Sigma Aldrich, Steinheim, Germany) diluted in a 0.14M sodium cacodylate trihydrate (Cacodylic acid sodium salt, Sigma Aldrich, Steinheim, Germany) buffer solution. After fixation, ASCs were stained with MB solution (1% M9140 Methylene Blue (certified by BSC, Sigma Aldrich, Steinheim, Germany) in borax (B-3545 Borax (99.5–05%), Sigma Aldrich, Steinheim, Germany)), rinsed with DPBS to eliminate the excess of MB, and visualized using light microscopy (Eclipse E600, Nikon). The captured images were processed using Matrix Vision software (Matrix Vision GmbH, Germany).

For DNA quantification at days 1, 3 and 7, cell-seeded scaffolds were washed with DPBS and placed in a new 24-well plate before adding 0.25 mL of 0.1% Triton-X100 solution for cell lysis. Total DNA content was measured according to the manufacturer's protocol (CyQuant Cell Proliferation Assay Kit, Invitrogen) using a fluorescent plate reader (TECAN Safire2, Switzerland).

Results and Discussion

Figure 1 presents SEM images of the PCL scaffolds surface reported earlier.[20]

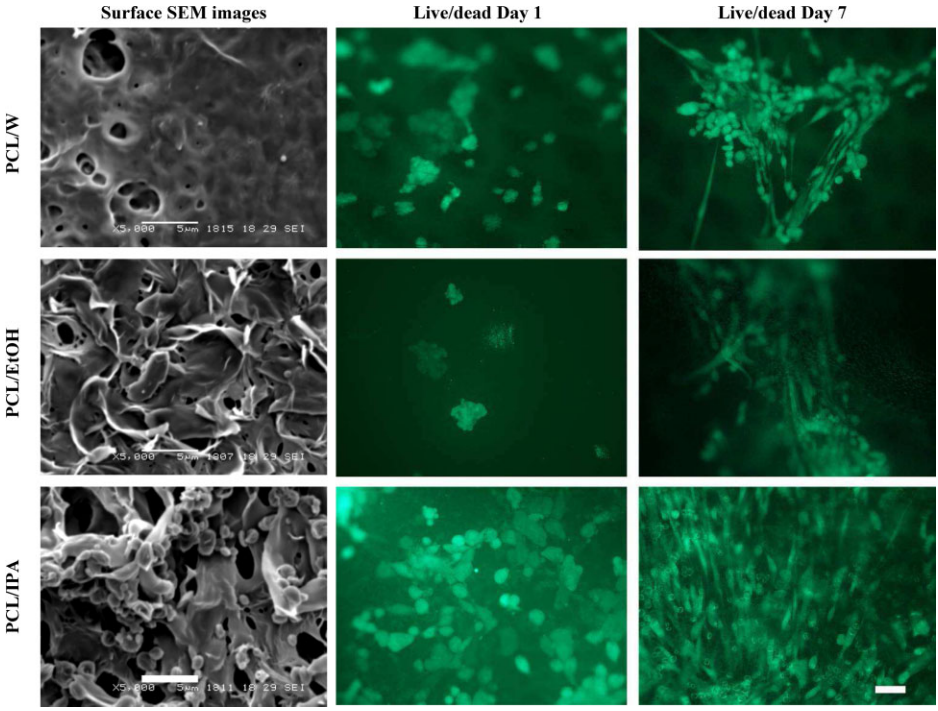

Figure 1.
SEM surface images (scale bar 5 μm) and Live/dead assay pictures on day 1 and 7 (Scale bar 50 μm) for PCL/W, PCL/EtOH and PCL/IPA scaffolds.

There, we demonstrated that the phase inversion allows tailoring of the surface morphology by using different coagulation baths affecting the characteristics of the solvent/polymer/non-solvent phase solubility.[17] A progressive increase of surface roughness seems to occur in the sequence PCL/W < PCL/EtOH < PCL/IPA. The PCL/W scaffold, in contrast to PCL/EtOH and PCL/IPA, presented a dense layer typical of fast phase inversion. The abundance of pores on the surface of the scaffolds increased in the sequence PCL/W < PCL/EtOH < PCL/IPA. The average pore size of PCL/IPA is 1.6 ± 1.2 μm in the cross section of the scaffold, in agreement with the range of the pore size (0.5–.5 μm) determined previously.[20] The PCL/EtOH and PCL/IPA scaffolds have high and interconnected porosity resulting in high water permeances (18.4 ± 4.3 and 24.8 ± 4.7 $m^3.m^{-2}.h^{-1}.bar^{-1}$,[20] respectively). Based on these values, the porosity of the PCL/IPA scaffold seems to be higher than that of the PCL/EtOH scaffold.

Figure 1 also shows hASC viability and attachment on the scaffolds at days 1 and 7. The live/dead images show that the cells are viable (green fluorescence) at both time points on all scaffolds. Interestingly, on the PCL/IPA scaffolds, the cells attach uniformly on the surface, in contrast to PCL/W and PCL/EtOH scaffolds, where they are sparsely attached. Also, cells seem to cluster on PCL/EtOH and PCL/W scaffolds indicating inhibited cell attachment. The images of MB staining at day 1 (Figure 2) are in agreement with live/dead imaging results and are further supported quantitatively by DNA content (Figure 3) at day 1. Lampin et al[14] suggested that the increase of surface roughness increases the hydrophobicity of the scaffold and that hydrophilic surfaces show better affinity for cells and lower affinity for proteins. Thus, increase the roughness can lead to higher protein adsorption on the scaffold surface. They also observed[14] that once proteins bind the surface, the roughness of the scaffold gets smoother again promoting cell attachment. According to this, the protein adsorption is expected to be stronger in the order of PCL/W < PCL/EtOH < PCL/IPA and the cells are expected to adhere better in the same order which is in agreement with the observed results of the current work.

The differences between the cell responses to the scaffold surface morphology were more pronounced at day 7. For the PCL/IPA scaffolds, hASCs grow as homogenous monolayer while on the PCL/W and PCL/EtOH scaffolds they form clusters and large parts of the surface are not covered with cells (Figures 1 and 2). Quantitative analysis of DNA content (Figure 3) shows that cell numbers are higher on PCL/IPA scaffolds compared to PCL/W and PCL/EtOH scaffolds at days 3 and 7. The slight decrease in cell number observed at day 7 compared to day 3 on PCL/IPA scaffolds may be due to the fact that cells reached the proliferation maximum already on day 3. The pore size ($\sim$ 1.5 μm) of the PCL/IPA scaffolds was too small to allow the penetration of hASCs in the scaffold. In fact, penetration of hASC into PCL hollow fiber (HF) scaffolds with a pore size of $\sim$ 32 μm have been found[17] although there, the cells did not form a uniform monolayer over the scaffold surface. Therefore, it seems that a compromise between pore size that allows cell spreading and scaffold colonization is desirable.

The highest proliferation rate of hASCs is observed on PCL/IPA, while on PCL/EtOH the proliferation rate is the lowest. Probably, the cells benefited from the better protein adsorption on PCL/IPA. Besides, this difference in hASC proliferation may be explained by the difference in scaffold surface porosity. It was previously observed, that a higher porosity of PCL scaffolds promoted proliferation and migration of fibroblast[10] and osteogenic[24] cells. The fibroblast cells aggregated on the PCL scaffolds with low porosity while spread uniformly on the higher porosity scaffolds.[10]

In summary, our results suggest that the obtained different surface morphologies, roughness, porosities and pore sizes of flat

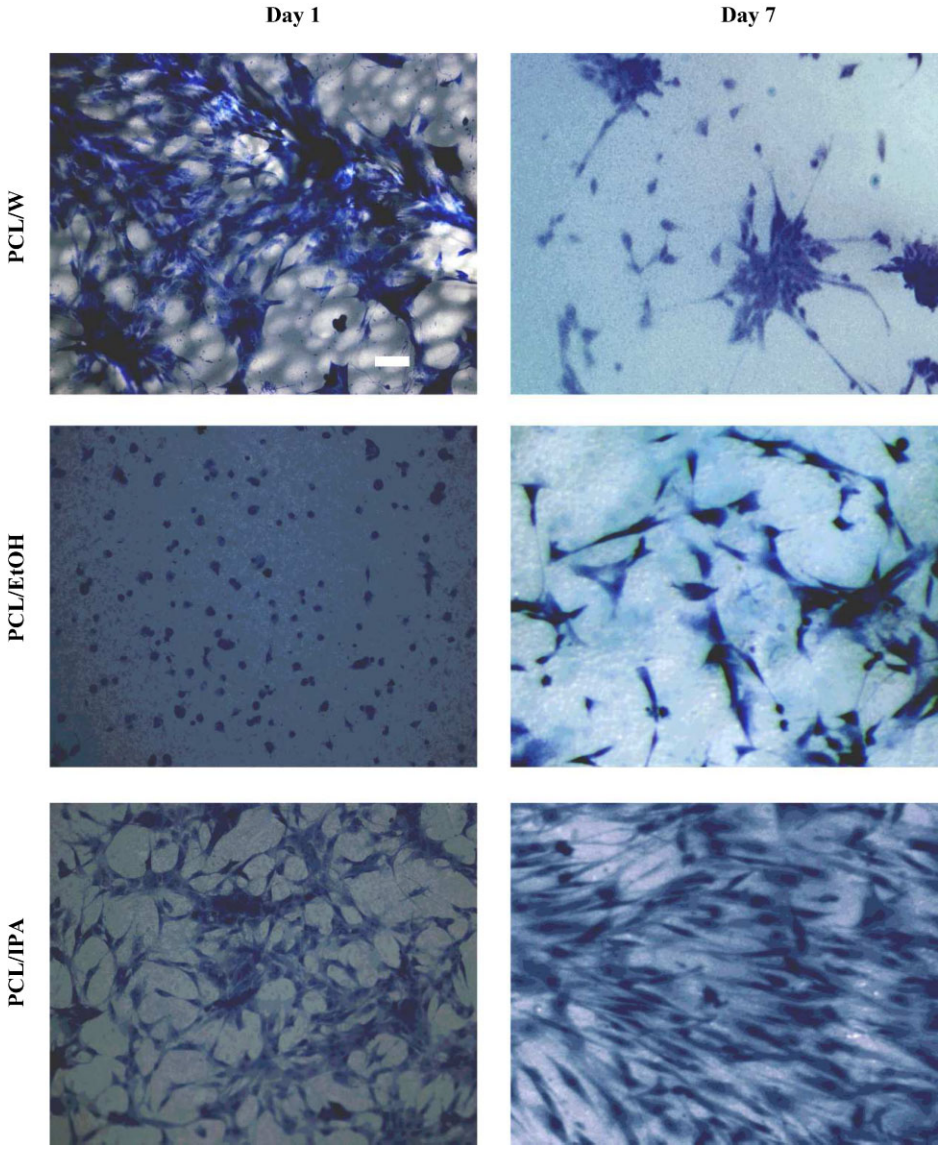

Figure 2.
Methylene Blue staining of PCL scaffolds on day 1 and 7. Scale bar 100 μm.

scaffolds have a strong effect on hASC response. Similarly, nano and microtopography have earlier shown to induce cues to affect cell adhesion and proliferation.[15,18,25] In contrast, the influence of roughness on cell response has been controversial. Gentile et al[25] found that cell adhesion and proliferation reach a maximum with moderate roughness, while for substrates presenting too high or low roughness cell adhesion and growth was limited. In our work, the scaffold with intermediate roughness (PCL/EtOH) induced a limited cell attachment, while the scaffolds with higher and lower roughness showed enhanced cell adhesion at day 1. However, only high roughness favours uniform cell attachment. To better

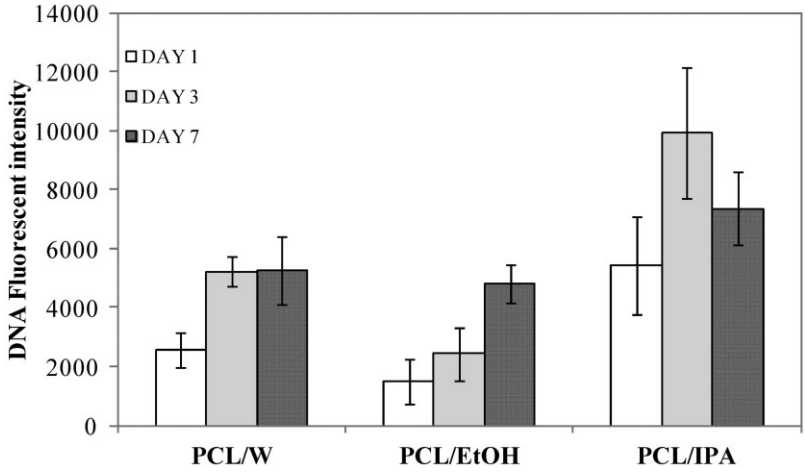

Figure 3.
DNA fluorescent intensity results for the different PCL flat scaffolds on days 1, 3, 7. The data are expressed as the mean ± SD.

understand the qualitative results observed here we would need to perform more studies in the future.

The PCL/IPA surface morphology induced the best cell response. The translation of this morphology to a three-dimensional (3D) scaffold, for instance in the shape of a HF, is desirable. A continuous PCL HF prepared by a phase inversion spinning technique, can be processed by tuning the process variables.[17] However, the surface morphology of the flat PCL/IPA scaffolds presented here, was not reproduced on the HFs fabricated using IPA as coagulation bath. Future work should focus on this direction.

Conclusion

The preliminary results of the effect of the surface morphology of the flat PCL scaffolds on the response of seeded hASCs, confirmed the importance of this parameter in the design of synthetic structures for different TE applications. From the three flat scaffolds fabricated by phase inversion, PCL/IPA scaffolds had suitable morphology (high roughness and porosity) for promoting good cell adhesion and proliferation. Further efforts on the translation of this morphology to 3D scaffolds and optimizing the pore size of the scaffolds to facilitate cell colonization are recommended.

Acknowledgements: The authors would like to thank the Spanish Ministry of Education (EX2009–049) and the Academy of Finland for granting postdoctoral fellowships to N.D. and S.H., respectively.

[1] J. D. Kretlow, A. G. Mikos, *AIChE J.* **2008**, *24*, 3048.
[2] Y. Wang, X.-L. Jiang, S.-C. Yang, X. Lin, Y. He, C. Yan, L. Wu, G.-O. Chen, Z.-Y. Wang, Q. Wu, *Biomaterials.* **2011**, *32*, 9207.
[3] R. Truckenmüller, S. Giselbrecht, M. Escalante-Marun, M. Groenendijk, B. Papenburg, N. Rivron, H. Unadkat, V. Saile, V. Subramaniam, A. van de Berg, C. van Blitterswik, M. Wessling, M. J. de Boer, D. Stamatialis, *Biomed. Microdevices.* **2012**, *14*, 95.
[4] B. J. Papenburg, L. Vogelaar, L. A. M. Bolhuis-Versteeg, R. G. H. Lammertink, D. Stamatialis, M. Wessling, *Biomaterials.* **2007**, *28*, **1998**.
[5] B. J. Papenburg, L. A. M. Bolhuis-Versteeg, D. W. Grijpma, J. Feijen, M. Wessling, D. Stamatialis, *Acta Biomater.* **2010**, *6*, 2477.
[6] D. C. Miller, A. Thapa, K. M. Haberstroch, T. J. Webster, *Biomaterials.* **2004**, *25*, 53.
[7] J. W. Calvert, K. G. Marra, L. Cook, P. N. Kumta, P. A. DiMilla, L. E. Weiss, *J. Biomed. Mater. Res.* **2000**, *52*, 279.
[8] J. Hao, Y. Liu, S. Zhou, Z. Li, X. Deng, *Biomaterials.* **2003**, *24*, 1531.

[9] F. J. O'Brien, B. A. Harley, I. V. Yannas, L. J. Gibson, *Biomaterials*. **2005**, *26*, 433.
[10] Q. Zhang, Y. Jiang, Y. Zhang, Z. Ye, W. Tan, M. Lang, *Polym. Degrad. Stab*. **2013**, *98*, 209.
[11] T.-W. Chung, D.-Z. Liu, S.-Y. Wang, S.-S. Wang, *Biomaterials*. **2003**, *24*, 4655.
[12] T.-W. Chung, S.-S. Wang, Y.-Z. Wang, C.-H. Hsieh, E. Fu, *J. Mater. Sci. : Mater. Med*. **2009**, *20*, 397.
[13] A. Thapa, T. J. Webster, K. M. Haberstroh, *J. Biomed. Mater. Res. A*. **2003**, *67*, 1374.
[14] M. Lampin, R. Warocquier-Clerout, C. Legris, M. Degrange, M. F. Sigot-Luizard, *J. Biomed. Mater Res*. **1997**, *36*, 99.
[15] M. J. Dalby, D. Giannaras, M. O. Riehle, N. Gadegaard, S. Affrossman, A. S. G. Curtis, *Biomaterials*. **2004**, *24*, 77.
[16] N. Diban, S. Haimi, L. Bolhuis-Versteef, S. Teixeira, S. Miettinen, A. Poot, D. Grijpma, D. Stamatialis, *Acta Biomater*. **2013**, Article in press DOI: 10.1016/j.actbio.2013.01.005.
[17] N. Diban, S. Haimi, L. Bolhuis-Versteef, S. Teixeira, S. Miettinen, A. Poot, D. Grijpma, D. Stamatialis, *J. Membr. Sci*. **2013**, *438*, 29.
[18] H.-Y. Chiang, H.-F. Chien, H.-H. Shen, J.-D. Yang, Y.-H. Chen, J.-H. Chen, S.-T. Hsieh, *J. Neuropathol. Exp. Neurol*. **2005**, *64*, 576.
[19] B. Nottelet, E. Pektok, D. Mandracchia, J.-C. Tille, B. Walpoth, R. Gurny, M. Möller, *J. Biomed. Mater. Res. A*. **2009**, *89*, 865.
[20] N. Diban, D. Stamatialis, *Macromol. Symp*. **2011**, *309/310*, 93.
[21] P. A. Zuk, M. Zhu, P. Ashjian, D. A. De Ugarte, J. I. Huang, H. Mizuno, Z. C. Alfonso, J. K. Fraser, P. Benhaim, M. H. Hedrick, *Mol. Biol. Cell*. **2002**, *13*, 4279.
[22] C. Wang, S. Yin, L. Cen, Q. Liu, W. Liu, Y. Cao, L. Cui, *Tissue Eng. Part A*. **2010**, *16*, 1201.
[23] M. Konno, T. S. Hamazaki, S. Fukuda, M. Tokuhara, H. Uchiyama, H. Okazawa, H. Okochi, M. Asashima, *Biomchem. Biophys. Res. Commun*. **2010**, *400*, 461.
[24] M. E. Gomes, H. L. Holtorf, R. L. Reis, A. G. Mikos, *Tissue Eng*. **2006**, *12*, 801.
[25] F. Gentile, L. Tirinato, E. Battista, F. Causa, C. Liberale, E. M. di Fabrizio, P. Decuzzi, *Biomaterials*. **2010**, *31*, 7205.

